Effects of stretch and thermal radiation on difluoromethane/air burning velocity measurements in constant volume spherically expanding flames*

Robert. R. Burrell, John L. Pagliaro, and Gregory T. Linteris

Energy and Environment Division
National Institute of Standards and Technology, Gaithersburg, Maryland 20899, USA

Corresponding Author:

Robert Burrell
Mailstop 8631
Energy and Environment Division
National Institute of Standards and Technology
Gaithersburg, Maryland 20899, USA
Phone: 301-975-2748
Email: robert.burrell@nist.gov

Colloquium Topic Area: Fire Research

Manuscript ID: PROCI-D-17-01593

Total length:	5777 words
Main text:	3455 words (MSWord 2016 word count)
Eq. 1:	[2 eqn lines + 2] x 7.6 words/line x (1 columns) = 30 words
Eq. 2:	[2 eqn lines + 2] x 7.6 words/line x (1 columns) = 30 words
Eq. 3:	[2 eqn lines + 2] x 7.6 words/line x (1 columns) = 30 words
Eq. (total):	90 words
References:	(37 references + 2) x (2.3 line/reference) x (7.6 words/line) = 681 words
Figure 1:	[67 mm + 10 mm] x 2.2 words/mm x 2 columns + (30 words in caption) = 369 words
Figure 2:	[67 mm + 10 mm] x 2.2 words/mm x 1 columns + (62 words in caption) = 231 words
Figure 3:	[67 mm + 10 mm] x 2.2 words/mm x 2 columns + (31 words in caption) = 370 words
Figure 4:	[67 mm + 10 mm] x 2.2 words/mm x 2 columns + (48 words in caption) = 387 words
Figure 5:	[67 mm + 10 mm] x 2.2 words/mm x 1 columns + (25 words in caption) = 194 words
Figure (total):	1551 words

This manuscript does not require color printing.

Accepted for publication in Proceedings of the Combustion Institute, Vol. 37. https://doi.org/10.1016/j.proci.2018.06.018
Presented at the 37th International Symposium on Combustion, Dublin, Ireland, July 29- August 3, 2018.

Effects of stretch and thermal radiation on difluoromethane/air burning velocity measurements in constant volume spherically expanding flames

Robert. R. Burrell, John L. Pagliaro, and Gregory T. Linteris

Energy and Environment Division
National Institute of Standards and Technology, Gaithersburg, Maryland 20899, USA

Abstract

Compared to current refrigerants, next-generation refrigerants are more environmentally benign but more flammable. The laminar burning velocity is being used by industry as a metric to screen refrigerants for fire risk, and it is also used for kinetic model development and validation. This study reports measurements of difluoromethane/air flame burning velocities for equivalence ratios from 0.9 to 1.4 in a spherical, constant volume device. Experimental burning velocities produced with the aid of an optically thin radiation model are about 17 % greater than those obtained with an adiabatic model. Characterization of flame stretch based on the product of Markstein and Karlovitz numbers indicates that while many experimental data are nearly stretch-free, those for slower burning velocities, smaller flame radii, and leaner conditions may not be. Limiting the data to regions estimated to be stretch-free requires extrapolation away from the experimental conditions to extract burning velocities near ambient conditions, e.g., at (298 K, 101 kPa). Lower uncertainty, desirable for kinetic model validation, is obtained by interpolating between experimental conditions, e.g., at (400 K, 304 kPa). Since thermal radiation and flame stretch were found to affect the inferred burning velocities of difluoromethane/air constant volume spherical flames, they should also be considered during data reduction of other mildly flammable refrigerants.

Keywords:

Refrigerant flammability, burning velocity, difluoromethane, thermal radiation, flame stretch

1. Introduction

Due to their high global warming potential (GWP), hydrofluorocarbon refrigerants in vapor-compression equipment are being phased down [1]. Replacement compounds with lower GWP are being developed, but the properties that allow them to react in the troposphere and maintain low GWP (typically adding H atoms or double carbon bonds) also make them mildly flammable. Flammable refrigerants are a new concern for the heating, ventilating, air-conditioning and refrigerating (HVAC&R) industry; characterizing the fire risk of these new agents is of high interest and the subject of recent study (e.g., [2]). There is a need to both rank the flammability of new agents and understand their full-scale fire behavior. The HVAC&R industry has adopted the burning velocity (S_u) as one flammability metric [3], which is reasonable since S_u affects flame stabilization, the rate of pressure rise in confined flame propagation, and is used in turbulent premixed combustion models.

Industry has an urgent need for a reliable S_u screening method for refrigerant/air flames. Defining such a method is made more challenging by the low S_u values for the refrigerant/air flames of interest, often between 1 cm/s to 10 cm/s. The American Society of Heating, Refrigerating and Air-Conditioning Engineers (ASHRAE) Standard 34 [3] specifies flammability Class 2L based on measured S_u less than 10 cm/s. These flames propagate at slow speeds similar to those of near-limit methane/air flames despite producing high flame temperatures similar to stoichiometric methane/air flames.

Difluoromethane (R-32, CH_2F_2) exhibits prototypical refrigerant/air flammability behavior and is selected for study in the present work. It is used as a pure working fluid or in blends, e.g., R410A is a 50/50 mass blend of R-32 and R-125 (C_2HF_5). The 100-year GWP of R-32 (GWP = 677) is lower than R-125 (GWP = 3170) but higher than R-1234yf (CH_2CFCF_3, GWP < 1) [4]. A peak S_u for R-32/air flames at ambient conditions is currently defined to be 6.7 cm/s in the ASHRAE flammability standard [3]. Thus, it is important to have accurate CH_2F_2/air S_u measurements.

The present experimental approach employs outwardly propagating spherical flames in a constant volume device with S_u calculated from the measured pressure rise and a thermodynamic flame model (e.g., [5-10]). Other methods used with refrigerants include: flame propagation in a vertical tube [11, 12]; constant pressure method outwardly propagating spherical flames (e.g., [13, 14]); and steady flow, nozzle-stabilized flames (e.g., [15]). Each has advantages and disadvantages as a standard test method. For instance, the tube method is subject to unquantified buoyancy, wall, and stretch effects [16]. The nozzle burner cannot be used for low burning velocities and consumes large quantities of reactants. The constant pressure spherical flame method requires relatively expensive optical equipment. The constant volume spherical flame method (e.g., [10]) uses small quantities of reactants, produces little product gas (which can contain up to 30 % HF by volume in CH_2F_2/air flames), and requires relatively inexpensive equipment. Spherically expanding flames are widely used to measure S_u of hydrocarbon/air mixtures for which the effects of buoyancy (e.g., [13, 17]), thermal radiation (e.g., [18-22]), and flame stretch (e.g., [20, 21, 23-26]) have been recent topics of research.

An important additional use for experimental burning velocity data is for kinetic model development and validation (e.g., [27]). For this purpose, it is the convention to use the laminar burning velocity (S_u^0) defined as the propagation speed into unburned reactants of a flame that is adiabatic, laminar, one-dimensional, steady, and stretch-free [28]. Small experimental uncertainty in S_u^0 is needed to properly constrain kinetic model rate parameters.

The present work investigates the role of radiation and stretch on the values of S_u and S_u^0 determined in spherical, constant volume method CH_2F_2/air flames. Using both constant volume and constant pressure spherical flame methods, Takizawa et al. [13] found that, for stoichiometric or rich flames, normal and micro-gravity CH_2F_2/air flame propagation measurements agree for values of $S_u^0 > 5$ cm/s. Since all S_u^0 values presently measured exceed this limit, buoyancy was not further considered.

2. Experimental approach

Measurements were performed using the 15.14 cm inner diameter stainless steel spherical chamber described in Refs. 7 and 8. Reactants were CH_2F_2 (Honeywell, Genetron 32, 99.9 % purity), argon (Messer Group, 99.995 % purity), oxygen (Air Products, 99.5 % purity), and house air treated with a 0.01 μm filter, a carbon filter, and a desiccant bed to remove small aerosols, organic vapors, and water vapor; final relative humidity in the air was typically less than 2 % [8]. After evacuating the chamber to less than 67 Pa for at least 5 minutes, reactants were added via partial pressures using an absolute pressure transducer (Omega PX811) calibrated against a heated absolute pressure capacitance manometer (Baratron 627D) with a reading accuracy of 0.12 %. Mixture initial temperature (T_i) was between 295 K and 299 K, and initial pressure (P_i) was between 87.9 kPa (660 torr) and 115 kPa (860 torr). Mixtures were given 5 minutes to settle and were then centrally ignited by a spark powered by a 100 nF capacitor bank charged to 13 kV. Pressure rise in the chamber was measured at 20 kHz using a piezoelectric pressure sensor (PCB Piezotronics 101A06) with a resolution of 0.07 kPa, a range of 3450 kPa, and a claimed accuracy of ±3.5 kPa.

Previous uncertainty analysis for this experimental system [8] suggests relative uncertainties in the initial mixture of about 1 % in the fuel/air equivalence ratio (ϕ), and 0.3 % and 0.8 % in the partial pressure of air and CH_2F_2, respectively. Relative uncertainty was 1.3 % in the dynamic pressure rise, 0.7 % in P_i, and 1 % in T_i. The maximum combined relative uncertainty at low S_u for a single experimental S_u measurement is $\pm$12 %.

3. Data reduction

Inferring S_u from a measured pressure (P) - time (t) trace employs the data reduction procedures summarized in Fig. 1. First, $P(t)$ is measured and noise is suppressed with cubic smoothing splines selected to ensure unstructured fit residuals over the useful range of data. The range of smoothed $P(t)$ is narrowed: data at early times are eliminated for $P(t) < 1.25P_i$, which is sufficient to remove ignition transients and electrical noise; data at longer times are eliminated beyond the maximum 2nd derivative of the pressure trace, which has been suggested as a marker for when the flame begins to interact with the chamber walls [29]. Second, the relationship between the unburned/burned gas thermodynamic states and the flame radius (R_f) was computed via the Hybrid ThermoDynamic-Radiation (HTDR) model [9] with species thermodynamic data taken from the NIST HFC mechanism [30]. Finally, the measured $P(t)$ and modeled $R_f(P)$ are combined to reconstruct S_u and the flame stretch rate (K).

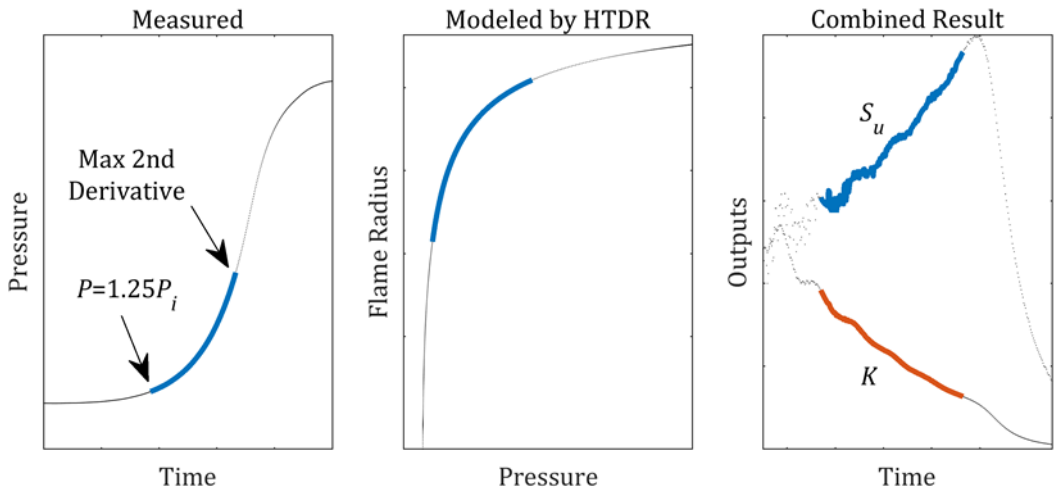

Figure 1: Data reduction process. A measured pressure trace (left) is smoothed, cropped, and combined with (center) the modeled flame radius to generate (right) flame burning velocity and stretch rate.

HTDR is a numerical, multi-zone, thermodynamic, spherically expanding flame model [9] which includes thermal radiation calculations based on RADCAL [31]. It assumes that the flame front is smooth, spherical, and infinitely thin; that no reactions occur in the unburned gas, which has uniform temperature

and composition; that the pressure is spatially uniform but evolves in time; that the unburned gas compression occurs isentropically; and that the burned gas is in chemical equilibrium at any instant. The model works by dividing the spherical domain into a series of shells and applying conservation of energy, mass, and volume. Starting from the center, an unburned shell is combusted by allowing it to reach equilibrium at constant pressure and enthalpy, causing increased volume and temperature. Equilibrium is then re-computed for all inner (burned) shells. Next, if radiation is enabled, all burned shells radiate at constant pressure, causing decreased volume and temperature. Finally, all shells are simultaneously, isentropically compressed to match the chamber volume. From this, the functional relationship for flame radius $R_f(P)$ is obtained.

From the measured $P(t)$ and modeled $R_f(P)$, the inferred S_u is calculated based on the result of Fiock and Marvin for a constant volume spherically expanding flame [32]:

$$S_u = \frac{\mathrm{d}R_f}{\mathrm{d}t} - \frac{\left({R_w}^3 - {R_f}^3\right)}{3{R_f}^2 \gamma_u P}\frac{\mathrm{d}P}{\mathrm{d}t} \tag{1}$$

where γ_u is the unburned gas specific heat ratio and R_w is the chamber radius. Using the chain rule, $\mathrm{d}R_f/\mathrm{d}t$ is evaluated via the product $\left(\mathrm{d}R_f/\mathrm{d}P\right)(\mathrm{d}P/\mathrm{d}t)$. The terms in Eq. (1) can be defined as $S_u = S_f - S_g$, which shows that S_u is computed from the difference of the total flame front velocity relative to the chamber center point ($S_f = \mathrm{d}R_f/\mathrm{d}t$) and the velocity due to gas expansion from heat release (S_g).

At each equivalence ratio (ϕ) tests were conducted at multiple P_i (typically three) between 87.9 kPa and 115 kPa. Each test is assumed to evolve in time along an isentrope in (T_u, P) space, where T_u and P are the unburned gas temperature and pressure, and S_u is obtained from Eq. (1). As done in the past (e.g., [33]), the experimental S_u curves are fitted with a power law surface ($\widehat{S_u}$) of the form:

$$\widehat{S_u}(T_u, P) = S_{u,ref}\left(\frac{T_u}{T_{ref}}\right)^a \left(\frac{P}{P_{ref}}\right)^b \tag{2}$$

where $S_{u,ref}$ is the value of surface $\widehat{S_u}$ at a reference state (T_{ref}, P_{ref}) and the exponents a and b are determined during fitting. Figure 2 shows the three experimental S_u curves, corresponding $\widehat{S_u}$ surface fit,

and projections of S_u on each coordinate plane for CH_2F_2/air with $\phi = 1.1$, assuming adiabatic conditions in the burned gas. Each S_u curve corresponds to one measured $P(t)$ trace with P_i = 87.9 kPa, 101 kPa, or 115 kPa. Using the surface fit $\widehat{S_u}$, values for S_u can be obtained at arbitrary (T_u, P), not just along the measured isentropes. For example, Fig. 2 shows, in the (T_u, P) plane, the locations of the two states, (298 K, 101 kPa) and (400 K, 304 kPa), for which experimental S_u^0 values are reported in the present work. Caution is advised when selecting (T_u, P) which require extrapolation far from the experimental isentropes as additional uncertainty will be introduced. For example, $\widehat{S_u}$(298 K, 101 kPa) in Fig. 2 is an extrapolation over about 30 K and 25 kPa but $\widehat{S_u}$(400 K, 304 kPa) is an interpolation between P_i = 87.9 kPa and 101 kPa experimental isentropes.

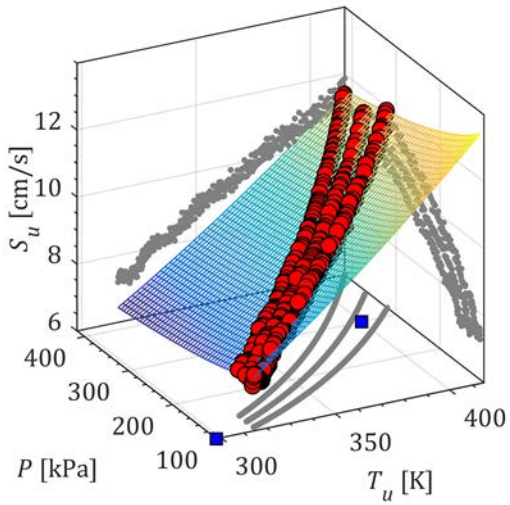

Figure 2: Example data set and fitted power law surface for CH_2F_2/air at $\boldsymbol{\phi = 1.1}$. Experimental $\boldsymbol{S_u}$ curves are marked as red circles and their 2D projections in each coordinate plane as grey dots. Fitted $\boldsymbol{\widehat{S_u}}$ is shown as a mesh surface. Reference states (298 K, 101 kPa) and (400 K, 304 kPa) are marked on the $(\boldsymbol{T_u, P})$ plane as blue squares.

Thermal radiation affects spherically expanding flames in two ways [18]. Reduced temperatures within the reaction zone cause lower reactivity and reduced S_u. Also, the hot product gases radiating heat will contract as their mass density increases, causing the flame to propagate against a radially inward flow. RADCAL provides various models to account for radiation: adiabatic conditions (no radiation correction),

emission-only radiation at the optically thin limit without reabsorption, or optically thick narrow-band radiation with reabsorption. Calculation of narrow-band radiation emission/absorption is computationally expensive and requires parameters not well characterized for the species present in CH_2F_2 combustion. Therefore, $R_f(P)$ was modeled only for adiabatic and optically thin conditions with the understanding that results of the more rigorous reabsorption radiation model fall between these limits [22]. RADCAL already contains Planck mean absorption coefficients for CO, CO_2, H_2O, and CH_4, and values for HF as a function of temperature [34] were added.

Besides radiation, another major factor that can affect S_u is flame stretch. Williams [35] estimated the stretch rate in spherically expanding flames as $K = (2/R_f)(\mathrm{d}R_f/\mathrm{d}t)$. A nondimensional form of K is the Karlovitz number, $Ka = (\alpha/{S_u}^2)K$, where α is the mixture thermal diffusivity. In spherically expanding laminar flames, Ka is greatest at small R_f where the flame surface is strongly curved. In constant volume method flames, the rising pressure reduces α which also helps drive $Ka \to 0$ for larger R_f (e.g., [9]). If stretch affects the measured S_u, it is expected to be most prominent at smaller R_f.

Positive stretch in spherically expanding flames is known to impact S_u in two ways: through imbalanced diffusive flux of thermal energy leaving the flame compared to chemical enthalpy entering, called preferential diffusion, and through a ϕ shift caused by faster transport of the more mobile reactant into the flame, called differential diffusion [28]. Preferential diffusion is parameterized by the Lewis number ($Le = \alpha/D$) which is the ratio of a gas mixture's thermal diffusivity to mass diffusivity (D). For CH_2F_2/air flames, $Le > 1$ such that as stretch increases the flames diffuse heat away at a greater rate than chemical enthalpy is gained leading to reduced flame temperatures and S_u. Preferential diffusion causes a lean shift in CH_2F_2/air flames due to the lower mobility of CH_2F_2 compared to O_2.

Lewis number effects are reflected in the Markstein length ($\mathcal{L}$) which is nondimensionalized by the flame thickness (δ_f) to form a Markstein number ($Ma = \mathcal{L}/\delta_f$) for which $|Ma| \gg 0$ corresponds to flames with high sensitivity to stretch. A previous study [14] suggests that Ma is large and positive for lean

CH_2F_2/air flames, which exhibit a strong stretch response, and that Ma approaches zero in rich flames which exhibit weak stretch response. It is possible to calculate Ma values based on simplified theoretical models (e.g., [36]), but these values are expected to be instructive rather than accurate due to the simplifications and uncertainties involved. To estimate Ma values for CH_2F_2/air flames, computed values for C_3H_8/air mixtures were used as approximations (justified based on the comparable molecular weights of CH_2F_2 and C_3H_8). Although this constitutes a significant approximation, an uncertainty factor of 2 was assigned to Ma for the purposes of evaluating the sensitivity of results to presumed Ma values. This uncertainty factor was chosen to encompass Ma values computed by Matalon [36] for flames in air with a variety of fuel molecule types and molecular weights, from methanol to octane.

Knowing Ka and Ma, the effect of stretch in S_u measurements can be evaluated. For sufficiently small stretch rates, $S_u = S_u^0 - \mathcal{L}K$ [36], or in non-dimensional parameters:

$$S_u = \frac{S_u^0}{1 + MaKa} \tag{3}$$

such that CH_2F_2/air flames characterized by $MaKa \geq 0$ have $S_u \leq S_u^0$ while stretch-free flames characterized by $MaKa \approx 0$ produce $S_u \approx S_u^0$. Note that Eq. (3) suggests, in principle, that measured S_u can be corrected to recover unstretched S_u^0 for a given $MaKa$. In practice, $MaKa$ is not known with enough certainty to justify this approach. In the present work, an empirical tolerance of $MaKa \leq 0.005$ was selected for $S_u \approx S_u^0$, which imposed an additional constraint on the useable range of $P(t)$ relevant for stretch-free conditions.

4. Results and discussion

The inferred experimental S_u values are sensitive to the choice of radiation model used in data reduction. This is demonstrated on the left frame of Fig. 3 for experimental S_u values of CH_2F_2/air flames with $\phi = 1$ and $P_i = 101$ kPa. Values obtained assuming optically thin radiation in the burned gas are about 17 % greater than those assuming adiabatic conditions. As described previously [22], the results with narrow-band radiation fall between these two limits. Given the significant correction illustrated in Fig. 3, data reduction using a narrow-band radiation model is warranted, however, the required radiation parameters are not available for halogenated hydrocarbon species under combustion conditions.

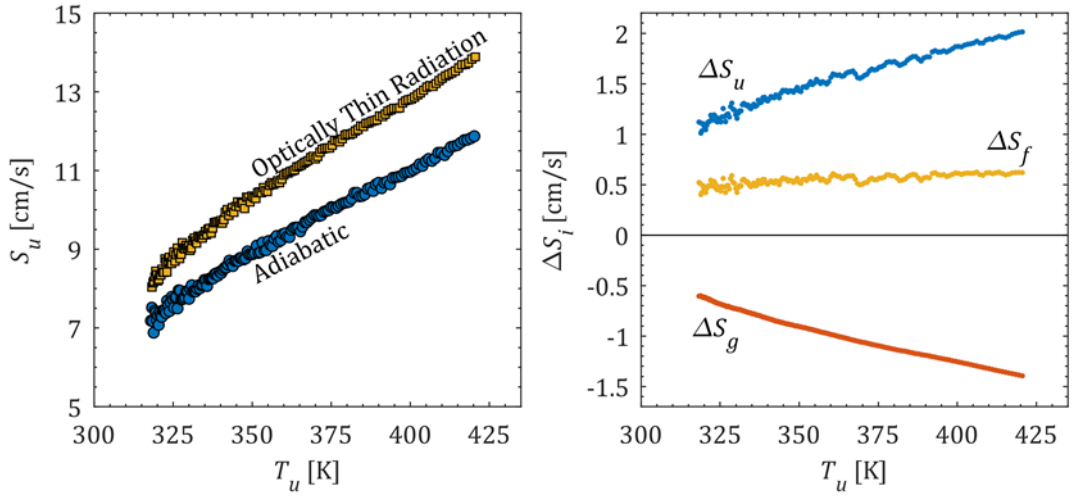

Figure 3: (Left) Comparison of experimental $\boldsymbol{S_u}$ values with and without thermal radiation for CH_2F_2/air at $\boldsymbol{\phi} = 1$ and $\boldsymbol{P_i} = 101$ kPa. (Right) Component contributions to the total difference in $\boldsymbol{S_u}$.

The reasons for the strong radiation effect are explored based on the terms of Eq. (1), i.e., $S_u = S_f - S_g$, in the right frame of Fig. 3. The total difference between S_u obtained using the optically thin and adiabatic models (ΔS_u) is decomposed into differences between total flame front velocity (ΔS_f) and gas expansion velocity (ΔS_g), i.e., $\Delta S_u = \Delta S_f - \Delta S_g$. Since the optically thin values are greater than the adiabatic ones, ΔS_u is positive for the present example, and of magnitude between 1 cm/s and 2 cm/s.

The greatest contribution is from ΔS_g which accounts for about 0.5 cm/s to 1.5 cm/s of the total difference, but at smaller R_f (i.e., low T_u) it is nearly matched in magnitude by $\Delta S_f \approx$ 0.5 cm/s. The burned gas thermal radiation influences the inferred S_u through reduced burned gas expansion velocity and greater total flame front velocity.

The impact of flame stretch on S_u should also be considered during data reduction, so that stretched flames are not included in the data reduction for S_u^0. Experimental values of S_u as a function of T_u, assuming adiabatic conditions, for CH_2F_2/air flames with $P_i = 101$ kPa and $\phi = 0.9$ and 1.3 are shown in Fig. 4 (left frame). In lean CH_2F_2/air flames, both differential and preferential diffusion cause reduced flame temperatures. In rich flames, the lean shift caused by preferential diffusion strengthens the flame and counteracts, to some extent, the weakening due to differential diffusion. These trends are illustrated in Fig. 4 (left frame), which shows that a greater range of rich flame data meets the empirical stretch-free criterion ($MaKa \leq 0.005$) than does lean flame data. For rich flames, about 2/3 of the data (corresponding to $T >$ 350 K) meet the stretch-free criterion, however, the power law fit to only "stretch-free" data also follows the remaining 1/3 of the data at lower T_u. Similar results were found for stoichiometric flames (not shown in Fig. 4). For lean flames, only about 1/4 of the data (i.e., $T_u >$ 365 K) meet the stretch-free criterion and the resulting power law fit to those "stretch-free" data overshoots the measurements at lower T_u by about 12 % at 315 K. Thus, for the lean flames, the surface fit parameters are sensitive to the choice of $MaKa$ threshold which results in additional uncertainty, especially when extrapolating far from the valid range of stretch-free data, e.g., to 298 K and 101 kPa. Moreover, power law fitting to all lean flame data (i.e., ignoring potential stretch restrictions) produced large fit residuals, an indication of poor fit quality. An alternative, as described below, is to use surface fitting to report S_u^0s at (T_u, P) conditions near those realized experimentally, e.g., 400 K and 304 kPa.

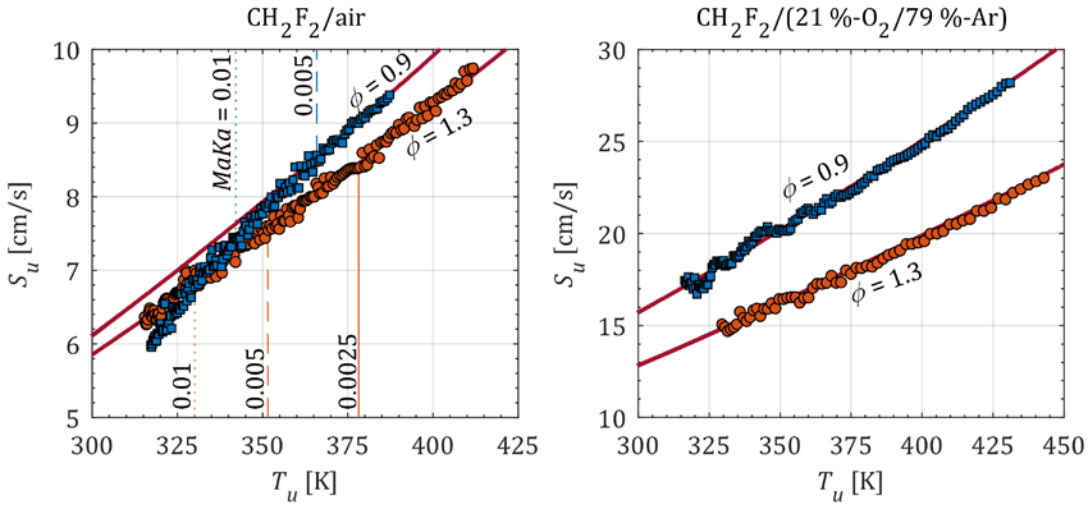

Figure 4: Comparison of lean and rich experimental $\boldsymbol{S_u}$ values assuming adiabatic conditions with $\boldsymbol{P_i} =$ 101 kPa for (left) CH_2F_2/air and (right) CH_2F_2/(21 %-O_2/79 %-argon) including projections of fitted $\widehat{\boldsymbol{S_u}}$ (thick red lines). Vertical line annotations on the left plot show the calculated locations of different stretch conditions.

Since the values of Ma used to eliminate stretch-affected data were a rough estimation based on propane, it is of value to explore stretch effects further. The importance of stretch can be reduced by using argon inert instead of nitrogen at the same reactant concentrations. Using argon modestly reduces α, which affects the mixture Lewis and Karlovitz numbers, but also substantially increases experimental S_u and K. Since $Ka \sim K/{S_u}^2$, the overall result is reduced Ka, and therefore $MaKa$, compared to flames in air. Experimental S_u for CH_2F_2/(21 %-O_2/79 %-argon) mixtures with $P_i = 101$ kPa and $\phi = 0.9$ and 1.3 are shown on the right of Fig. 4. Because of the reduced sensitivity to stretch, the empirical stretch-free criterion ($MaKa \leq 0.005$) is met by all data for both values of ϕ. Both lean and rich S_u^0 curves closely follow their fitted power law curves, and there is less uncertainty in extrapolating to 298 K and 101 kPa.

The variation of S_u^0 with ϕ is presented in Fig. 5 for flames in air. The lower curves show results for flames at (298 K, 101 kPa) and the upper curves at (400 K, 304 kPa). For each temperature/pressure condition, results are shown for data reduction assuming adiabatic conditions (ADI) and assuming radiative heat losses at the optically thin limit (OTL). At (298 K, 101 kPa), the OTL S_u^0 values are about 17 % higher than ADI values, while for flames at (400 K, 304 kPa), the OTL S_u^0 values are 17 % to 23 % greater than the ADI values. For comparison, the data of Takizawa et al. [33] are also presented (x

symbols), and these agree well with the present data reduced with the adiabatic model (which was the same assumption used in Ref. 33). Data from Moghaddas et al. [37] are also presented at (400 K, 304 kPa), and these agree with the present ADI data and those of Ref. 33 for $\phi \geq 1.2$, but are higher as ϕ decreases. Reasons for this remain unclear, although differences in stretch correction or in data reduction techniques are possibilities.

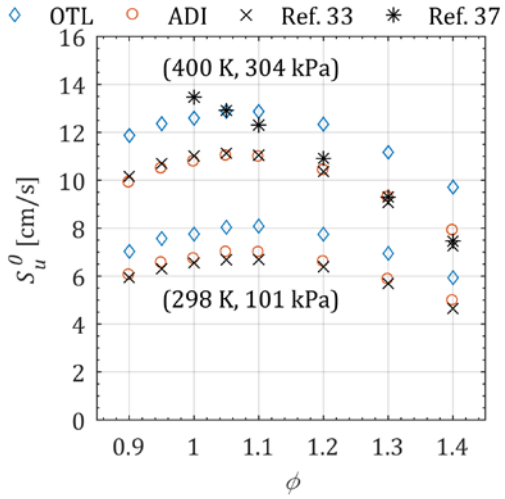

Figure 5: Comparison of experimental $\boldsymbol{S_u^0}$ values for CH_2F_2/air flames obtained with adiabatic (ADI) and optically thin (OTL) thermal radiation models along with literature values.

5. Concluding remarks

Burning velocities of difluoromethane/air and difluoromethane/oxygen/argon flames were measured in a constant volume, outwardly-propagating, spherical flame experiment, with initial conditions near ambient and for equivalence ratios from 0.9 to 1.4. Data reduction of the measured pressure traces was analyzed to understand the effects of burned gas thermal radiation and flame stretch. For unburned gases at 298 K and 101 kPa, modeling the burned gas thermal radiation at the optically thin limit increased the inferred burning velocities in air by about 17 % compared to those inferred with an adiabatic model. This was due to reduced burned gas expansion velocity and greater total flame front velocity when including the radiative heat losses. More sophisticated, and potentially more accurate, radiation reabsorption calculations require infrared absorption spectra data at combustion-relevant temperatures and pressures which are not presently available. The role of flame stretch on burning velocity was parameterized by the product of Markstein and Karlovitz numbers. The data for stoichiometric and rich flames was estimated to be essentially stretch-free for most of the conditions presented, however, lean flames may be influenced by stretch at smaller radii. Moreover, producing laminar burning velocities at unburned gas conditions of 298 K and 101 kPa from power law surface fits to the experimental burning velocities requires extrapolation which introduces larger uncertainty. In contrast, interpolating measured burning velocities to 400 K and 304 kPa avoids uncertainty due to extrapolations and may provide better quality data for kinetic model validation. To facilitate accurate assessment of refrigerant flammability and provide data suitable for kinetic model development and optimization, data reduction procedures used to generate experimental burning velocities should be scrutinized.

Acknowledgements

This work was supported by the Buildings Technologies Office of the U.S. Department of Energy, Office of Energy Efficiency and Renewable Energy under contract no. DE-EE0007615 with Antonio Bouza serving as Project Manager. Dr. Burrell was supported by a NRC-NIST postdoctoral research associateship.

References

[1] Further Amendment of the Montreal Protocol, UNEP/OzL.Pro.28/CRP/10, United Nations Environment Programme, Kigali, Rwanda, 2016.

[2] S. Kujak, ASHRAE J., 59 (5) (2017) 16-24.

[3] Designation and Safety Classification of Refrigerants, ANSI/ASHRAE Addendum ak to ANSI/ASHRAE Standard 34-2016, ASHRAE, Atlanta, GA, 2016.

[4] G. Myrhe, et al., Anthropogenic and Natural Radiative Forcing, Fifth Assessment Report of the Intergovernmental Panel on Climate Change, Cambridge University Press, 2013.

[5] M. Metghalchi, J.C. Keck, Combust. Flame, 38 (1980) 143-154.

[6] P.G. Hill, J. Hung, Combust. Sci. Technol., 60 (1-3) (1988) 7-30.

[7] J.L. Pagliaro, G.T. Linteris, P.B. Sunderland, P.T. Baker, Combust. Flame, 162 (1) (2015) 41-49.

[8] J.L. Pagliaro, G.T. Linteris, V.I. Babushok, Combust. Flame, 163 (2016) 54-65.

[9] C. Xiouris, T.L. Ye, J. Jayachandran, F.N. Egolfopoulos, Combust. Flame, 163 (2016) 270-283.

[10] M. Faghih, Z. Chen, Science Bulletin, 61 (16) (2016) 1296-1310.

[11] T. Jabbour, D.F. Clodic, ASHRAE Trans., 110 (2) (2004) 522-533.

[12] P. Papas, S. Zhang, W. Kim, S.P. Zeppieri, M.B. Colket, P. Verma, Proceed. Combust. Inst., 36 (1) (2017) 1145-1154.

[13] K. Takizawa, S. Takagi, K. Tokuhashi, S. Kondo, M. Mamiya, H. Nagai, ASHRAE Trans., 119 (2013) 243-254.

[14] J.L. Pagliaro, G.T. Linteris, Burning Velocities of Marginally Flammable Refrigerant-Air Mixtures, Spring Meeting of the Eastern States Section of the Combustion Institute, Princeton University, 2016.

[15] G.T. Linteris, ASHRAE Trans., 112 (2) (2006) 448-458.

[16] R.A. Strehlow, d.L. Reuss, Effect of a zero g environment on flammability limits as determined using a standard flammability tube apparatus, NASA-CR-3259, National Aeronautic and Space Administration, Washington, DC, 1980.

[17] B.C. Choi, J.S. Park, A.F. Ghoniem, Energy, 95 (2016) 517-527.

[18] Z. Chen, Combust. Flame, 157 (12) (2010) 2267-2276.

[19] H. Yu, W. Han, J. Santner, X.L. Gou, C.H. Sohn, Y.G. Ju, Z. Chen, Combust. Flame, 161 (11) (2014) 2815-2824.

[20] J. Jayachandran, R.H. Zhao, F.N. Egolfopoulos, Combust. Flame, 161 (9) (2014) 2305-2316.

[21] J. Jayachandran, A. Lefebvre, R.H. Zhao, F. Halter, E. Varea, B. Renou, F.N. Egolfopoulos, Proceed. Combust. Inst., 35 (2015) 695-702.

[22] Z. Chen, Proceed. Combust. Inst., 36 (2017) 1129-1136.

[23] Z. Chen, M.P. Burke, Y. Ju, Combust. Theor. Model., 13 (2) (2009) 343-364.

[24] A. Moghaddas, K. Eisazadeh-Far, H. Metghalchi, 159 (4) (2012) 1437-1443.

[25] Z. Chen, Combust. Flame, 162 (6) (2015) 2442-2453.

[26] F.J. Wu, W.K. Liang, Z. Chen, Y.G. Ju, C.K. Law, Proceed. Combust. Inst., 35 (2015) 663-670.

[27] F.N. Egolfopoulos, N. Hansen, Y. Ju, K. Kohse-Höinghaus, C.K. Law, F. Qi, Prog. Energy Combust. Sci., 43 (2014) 36-67.

[28] C.K. Law, Combustion Physics, Cambridge University Press, New York City, U.S.A., 2006.

[29] A. Omani, L. Tartakovsky, Combust. Flame, 168 (2016) 127-137.

[30] D.R. Burgess, M.R. Zachariah, W. Tsang, P.R. Westmoreland, Prog. Energy Combust. Sci., 21 (6) (1995) 453-529.

[31] W.L. Grosshandler, RADCAL: A Narrow-Band Model for Radiation Calculations in a Combustion Environment, NIST Technical Note 1402, National Institute of Standards and Technology, Gaithersburg, MD, 1993.

[32] E.F. Fiock, C.F. Marvin, Chem. Rev., 21 (3) (1937) 367-387.

[33] K. Takizawa, A. Takahashi, K. Tokuhashi, S. Kondo, A. Sekiya, Combust. Flame, 141 (3) (2005) 298-307.

[34] S.P. Fuss, A. Hamins, Trans. ASME, 124 (1) (2002) 26-29.

[35] F.A. Williams, A review of some theoretical considerations of turbulent flame structure, AGARD Conference Proceedings, AGARD-CP-164, NATO Science and Technology Organization, 1975.

[36] M. Matalon, Proceed. Combust. Inst., 32 (1) (2009) 57-82.

[37] A. Moghaddas, C. Bennett, E. Rokni, H. Metghalchi, HVAC&R Res., 20 (1) (2014) 42-50.